Biochemical and Biophysical Research Communications 438 (2013) 653–659

Contents lists available at ScienceDirect

Biochemical and Biophysical Research Communications

journal homepage: www.elsevier.com/locate/ybbrc

An in-cell NMR study of monitoring stress-induced increase of cytosolic Ca^{2+} concentration in HeLa cells

Dambarudhar Shiba Sankar Hembram [a], Takahiro Haremaki [a], Jumpei Hamatsu [a], Jin Inoue [a], Hajime Kamoshida [a], Teppei Ikeya [a], Masaki Mishima [a], Tsutomu Mikawa [b], Nobuhiro Hayashi [c], Masahiro Shirakawa [d], Yutaka Ito [a,*]

[a] Department of Chemistry, Graduate School of Science and Engineering, Tokyo Metropolitan University, 1-1 Minami-Osawa, Hachioji-shi, Tokyo 192-0373, Japan
[b] Cellular and Molecular Biology Unit, RIKEN Advanced Science Institute, Wako-shi, Saitama 351-0198, Japan
[c] Department of Life Science, Graduate School of Bioscience and Biotechnology, Tokyo Institute of Technology, 4259 B-1, Nagatsuda-chou, Midori-ku, Yokohama, Kanagawa 226-8501, Japan
[d] Department of Molecular Engineering, Graduate School of Engineering, Kyoto University, Nishikyo-ku, Kyoto 615-8510, Japan

ARTICLE INFO

Article history:
Received 19 July 2013
Available online 8 August 2013

Keywords:
In-cell NMR
HeLa cells
Cytosolic Ca^{2+} concentration
Calbindin D_{9k}

ABSTRACT

Recent developments in in-cell NMR techniques have allowed us to study proteins in detail inside living eukaryotic cells. The lifetime of in-cell NMR samples is however much shorter than that in culture media, presumably because of various stresses as well as the nutrient depletion in the anaerobic environment within the NMR tube. It is well known that Ca^{2+}-bursts occur in HeLa cells under various stresses, hence the cytosolic Ca^{2+} concentration can be regarded as a good indicator of the healthiness of cells in NMR tubes. In this study, aiming at monitoring the states of proteins resulting from the change of cytosolic Ca^{2+} concentration during experiments, human calbindin D_{9k} (P47M + C80) was used as the model protein and cultured HeLa cells as host cells.

Time-resolved measurements of 2D ^{1}H–^{15}N SOFAST–HMQC experiments of calbindin D_{9k} (P47M + C80) in HeLa cells showed time-dependent changes in the cross-peak patterns in the spectra. Comparison with *in vitro* assignments revealed that calbindin D_{9k} (P47M + C80) is initially in the Mg^{2+}-bound state, and then gradually converted to the Ca^{2+}-bound state. This conversion process initiates after NMR sample preparation. These results showed, for the first time, that cells inside the NMR tube were stressed, presumably because of cell precipitation, the lack of oxygen and nutrients, etc., thereby releasing Ca^{2+} into cytosol during the measurements. The results demonstrated that in-cell NMR can monitor the state transitions of stimulated cells through the observation of proteins involved in the intracellular signalling systems. Our method provides a very useful tool for *in situ* monitoring of the "healthiness" of the cells in various in-cell NMR studies.

1. Introduction

Since NMR was first applied to observe heteronuclear multidimensional NMR spectra of proteins inside *Escherichia coli* cells [1], this approach (in-cell NMR) has continued to be used as the only tool for investing protein behaviours in detail under molecular crowding [2] in the cytosol. In bacterial cells, in-cell NMR has contributed towards investigating conformational changes, dynamics, binding events and 3D structures [3–9]. In eukaryotic cells, studies have been reported using *Xenopus laevis* oocytes/eggs [10,11], *Pichia pastoris* [12], insect cells [13], and mammalian cells [14–16].

For in-cell NMR experiments it is definitely crucial to ensure that cells are alive during the measurements. The lifetime of in-cell NMR samples is however much shorter than that in culture media, presumably because cells are packed into a tiny space in an NMR tube, and various stresses as well as the lack of oxygen and nutrients can easily occur. In our previous studies, the maximum duration of in-cell NMR experiments was set such that cell viability is not less than ~85–90%, e.g., ~6 h for *E. coli* samples [5] and ~3 h for HeLa samples [14]. Although the short lifetime of samples is inevitable as long as we use standard NMR equipment and NMR tubes, it is nevertheless necessary to understand the conditions cells experience inside an NMR tube, in order to bring the experiments closer to "physiological" conditions. However, to the best

Abbreviations: HMQC, heteronuclear multiple quantum coherence; HSQC, heteronuclear single quantum coherence.

* Corresponding author. Fax: +81 42 677 2525.
E-mail address: ito-yutaka@tmu.ac.jp (Y. Ito).

0006-291X/$ - see front matter © 2013 Elsevier Inc. All rights reserved.
http://dx.doi.org/10.1016/j.bbrc.2013.07.127

of our knowledge, detailed investigations on this issue have not yet been reported.

The calcium ions (Ca^{2+}) are one of the most common signal transducers in eukaryotic cells [17–19]. Ca^{2+} may play a dual role as a messenger and a stressor in the process of cell damage, death and survival [20]. Influx of Ca^{2+} upon stimulation either from intracellular stress or through different types of Ca^{2+} channels leads to an increase in cytosolic Ca^{2+} concentration, which eventually triggers apoptosis [21,22]. For example, it is reported that prolonged stress forces endoplasmic reticulum (ER) to release calcium and induce cell death and ageing related diseases [23]. For this reason the cytosolic concentration of Ca^{2+} can be regarded as a good indicator of the healthiness of cells in NMR tubes.

Normal cytosolic Ca^{2+} levels exist at low concentrations of around ~100 nM, since it precipitates phosphate and controls a wide variety of cellular process such as cell-cycle progression, differentiation, muscle contraction, enzymatic activities and extracellularly, Ca^{2+} wave and cell morphology [24]. To maintain a low concentration, Ca^{2+} is actively pumped from the cytosol to the extracellular space and into the ER, and sometimes into the mitochondria [25]. Excess cytosolic Ca^{2+} can result in the enzymatic breakdown of proteins and cell death by stress.

Many cellular proteins bind Ca^{2+} tightly. In some cases they simply buffer free Ca^{2+}, thus lowering the cytosolic concentration. Others trigger second-messenger pathways [26]. It is believed that the calcium binds cooperatively to those proteins [27]. Calcium binding proteins can also bind Mg^{2+} with much less affinity. In contrast to Ca^{2+}, Mg^{2+} is a quite abundant divalent metal ion within cells (0.5–2.0 mM).

In this report, we demonstrated in-cell NMR in HeLa cells with the aim of monitoring cytosolic Ca^{2+} concentration during the experiments. We selected human calbindin D_{9k}, a small (79 residues) single domain EF-hand calcium binding protein, as the probe molecule to be investigated. Calbindin D_{9k} plays a role as a buffer protein which maintains the cytosolic Ca^{2+} concentration without other direct and significant activities [28], thus making it a suitable candidate for this study. In resting cells, where the free Ca^{2+} concentration is 1000-fold less than free Mg^{2+}, calbindin D_{9k} is in the Mg^{2+}-bound state. With an increase of cytosolic Ca^{2+} concentration, Mg^{2+} ions in calbindin D_{9k} are expected to be replaced by Ca^{2+}.

2. Materials and methods

2.1. Sample preparation

The DNA fragment encoding the human calbindin D_{9k} gene containing the proline-47 to methionine mutation and the C-terminal additional cysteine residue for the CPP^{TAT} conjugation [henceforth referred as calbindin D_{9k} (P47M + C80)] was synthesised. The P47M mutation was introduced so as to restrict *cis–trans* isomerisation [29]. The DNA fragment was inserted into a pET3a vector for overexpression in the *E. coli* BL21 Star (DE3) pLysS strain. Uniformly $^{13}C/^{15}N$-labelled samples were prepared by growing the bacteria in M9 medium containing $^{15}NH_4Cl$ and [$^{13}C_6$]-D-glucose. For the preparation of uniformly ^{15}N-labelled samples, [$^{13}C_6$]-D-glucose was replaced by unlabelled D-glucose. The lysine-selectively ^{15}N-labelled samples were prepared by using M9 medium containing 100 mg/L ^{15}N-lysine. Cells were grown at 37 °C, and protein expression was induced by the addition of isopropyl thio-β-D-thiogalactoside. After ~14 h of further growth, the cells were harvested. After re-suspending in the lysis buffer [20 mM imidazole (pH 7.0), 20 mM NaCl and 1 mM EDTA], the harvested cells were lysed by sonication. The cleared lysate was prepared by ultra-centrifugation, and then mixed with an equal amount of the pre-heated (95 °C) lysis buffer, and kept at 95 °C for 3 min. Precipitated proteins were removed by another ultra-centrifugation. The supernatant was then loaded onto a DEAE–Sepharose column pre-equilibrated with the lysis buffer. The column was washed with 5 column volumes of the same buffer, followed by elution with a linear gradient of 20–300 mM NaCl. The fractions containing calbindin D_{9k} (P47M + C80) were loaded onto a Superdex-75 16/60 column pre-equilibrated with the preparation buffer [20 mM Tris–HCl (pH 7.4), 20 mM NaCl, and 1 mM EDTA]. Further purification was carried out by Resource-Q column chromatography with a linear gradient of 0–200 mM NaCl.

2.2. Preparation of samples for backbone resonance assignments in vitro

The purified calbindin D_{9k} (P47M + C80), which was in the metal-free state, was concentrated (~2 mM) and dissolved in the NMR buffer [20 mM Tris–HCl (pH7.4), 150 mM NaCl, and 5 mM DTT]. For the preparation of samples in the Mg^{2+}- and Ca^{2+}-bound states, $MgCl_2$ and $CaCl_2$ solutions were added to the final concentration of 5 mM, respectively.

2.3. Preparation of in-cell NMR samples

The Ca^{2+}-bound calbindin D_{9k} (P47M + C80) was dissolved into PBS buffer prior to the incorporation into HeLa cells. For incorporation, we employed the procedure reported by Inomata et al. [14], in which the cell-penetrating peptide from HIV-1 TAT protein (CPP^{TAT}) was used. The concentration of calbindin D_{9k} (P47M + C80) in in-cell NMR samples was estimated by comparing the density of the Coomassie-stained bands in SDS–PAGE gels with those of purified calbindin D_{9k} (P47M + C80) with known concentration.

2.4. NMR measurement

NMR experiments were performed at 37 °C on a Bruker Avance III 600 MHz spectrometer equipped with a cryogenic TCI probehead. For in-cell NMR samples, sequential 2D $^{1}H–^{15}N$ SOFAST–HMQC [30] spectra were measured. A non-linear sampling scheme [31–33] was used for the indirectly observed ^{15}N-dimension to reduce experimental times to ~40 min. For each experiment, a total of 512 (t_2, $^{1}H^{N}$) × 16 (t_1, ^{15}N) complex points with 256 transients were acquired.

Backbone resonance assignments of metal-free, Ca^{2+}- and Mg^{2+}-bound calbindin D_{9k} (P47M + C80) *in vitro* were performed by analysing 3D CBCANH, CBCA(CO)NH, HN(CA)CO and HNCO spectra. A non-linear sampling scheme was used for the indirectly observed dimensions in order to reduce experimental times. Briefly, approximately 1/4 of the points were selected in a pseudo-random fashion from the conventional regularly spaced grid of t_1, t_2 points.

2.5. NMR data processing and analysis

For 2D NMR data, a 1D maximum entropy reconstruction was applied for the indirectly acquired ^{15}N-dimension after processing the directly acquired dimension by Fourier transformation using Azara v2.8 (W. Boucher, www.bio.cam.ac.uk/azara). For 3D NMR data, a 2D quantitative maximum entropy [13] reconstruction was applied for the indirectly acquired dimensions (t_1 and t_2) after processing the directly acquired dimension (t_3) by Fourier transformation.

All NMR spectra were analysed using the CcpNmr Analysis 2.2.2 software [34].

3. Results

3.1. ^{1}H–^{15}N SOFAST–HMQC spectra of human calbindin D_{9k} (P47M + C80) in HeLa cells

^{15}N-labelled calbindin D_{9k} (P47M + C80) in the Ca^{2+}-bound state was efficiently incorporated into HeLa cells (Fig. 1A). The concentration of calbindin D_{9k} (P47M + C80) in an in-cell NMR sample was estimated to be ~100 μM. Fig. 1B–F show a series of 2D ^{1}H-^{15}N SOFAST–HMQC spectra of uniformly ^{15}N-labelled calbindin D_{9k} (P47M + C80) in HeLa cells. Next we confirmed that the proteins observed in the spectra were indeed inside the living cells. Most ^{1}H–^{15}N correlation cross-peaks disappeared upon removal of the HeLa cells by gentle centrifugation after the measurements (Supplementary Fig. S1a), whereas the lysate of the harvested cells yielded a similar spectrum to the in-cell NMR spectrum (Supplementary Fig. S1b). These results demonstrated that the contribution of extracellular proteins to the observed signals is negligible. The viability of the HeLa cells after approximately 3.5 h of NMR measurements was confirmed to be 90 ± 3% by trypan-blue staining.

When comparing the sequential spectra (each took 38 min), time-dependent changes in the cross-peak pattern were apparently detected. We repeated the experiments employing the identical parameters, and found that these changes were reproducible (data not shown).

The ^{1}H–^{15}N correlation cross-peaks in each in-cell NMR spectrum were analysed in reference to the *in vitro* assignments. However, considering the overlap of cross-peaks in the in-cell NMR spectra, which is mainly caused by the line broadening due to increased viscosity in the cytosol and specific/nonspecific interactions with various intracellular factors, we anticipated difficulties in the assignment transfer process from the *in vitro* to the in-cell NMR data: solid assignments for isolated peaks, but highly ambiguous assignments for overlapped or significantly broadened peaks. Lysine-selectively ^{15}N-labelled calbindin D_{9k} (P47M + C80) was therefore prepared, aiming at simplifying the spectra, thus enabling the provision of more accurate assignments. Fig. 1G–K show a series of 2D ^{1}H–^{15}N SOFAST–HMQC spectra of lysine-selectively ^{15}N-labelled calbindin D_{9k} (P47M + C80) in HeLa cells.

3.2. Backbone resonance assignments of human calbindin D_{9k} (P47M + C80) in vitro

For the assignment transfer process, we needed to perform backbone resonance assignments for human calbindin D_{9k} (P47M + C80) *in vitro*, since no assignments have been done for this protein, even though detailed NMR studies have been reported for bovine [35,36] and porcine calbindin D_{9k} [37]. Backbone resonance assignments for the metal free, Mg^{2+}- and Ca^{2+}-bound states were summarised in Supplementary Figs. S2, S3 and S4, respectively. Chemical shift differences between these three states were mapped onto the homology-modelled 3D structure (PDB:1CLB) (Supplementary Fig. S5).

3.3. Time-dependent conversion from the Mg^{2+}- to the Ca^{2+}-bound states inside HeLa cells

Fig. 2A and C show the comparison of the 2D ^{1}H–^{15}N SOFAST–HMQC spectra of calbindin D_{9k} (P47M + C80) in HeLa cells in the

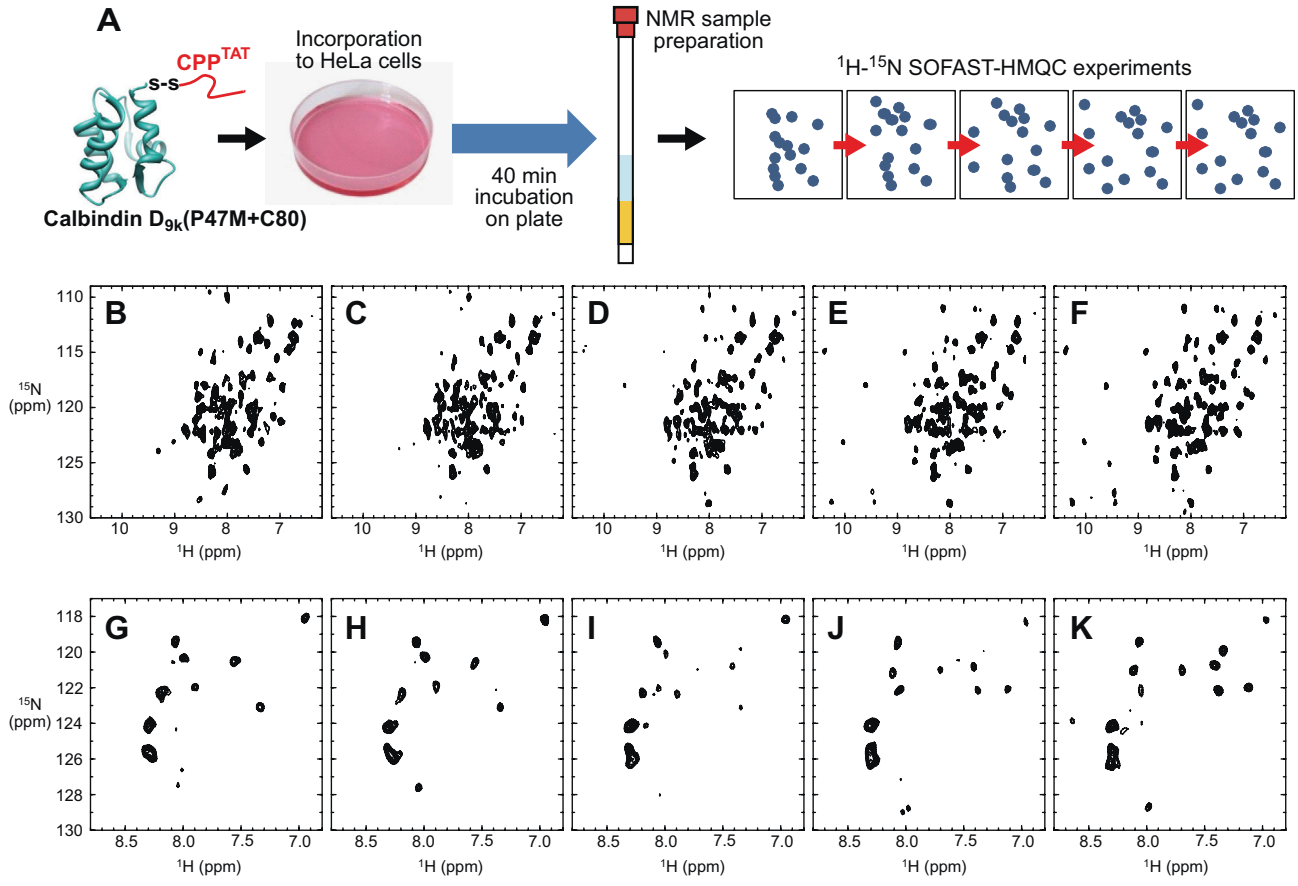

Fig. 1. (A) Schematic illustration of the in-cell NMR experiments of calbindin D_{9k} (P47M + C80) in HeLa cells. Time course of the 2D ^{1}H–^{15}N SOFAST–HMQC spectra of uniformly ^{15}N-labelled (B–F) and lysine-selectively ^{15}N-labelled (G–K) calbindin D_{9k} (P47M + C80) in HeLa cells. The spectra were obtained during the period of 0–38 min (B and G), 39–76 min (C and H), 77–114 min (D and I), 115–152 min (E and J), and 153 to 190 min (F and K) from the start of the in-cell NMR experiments.

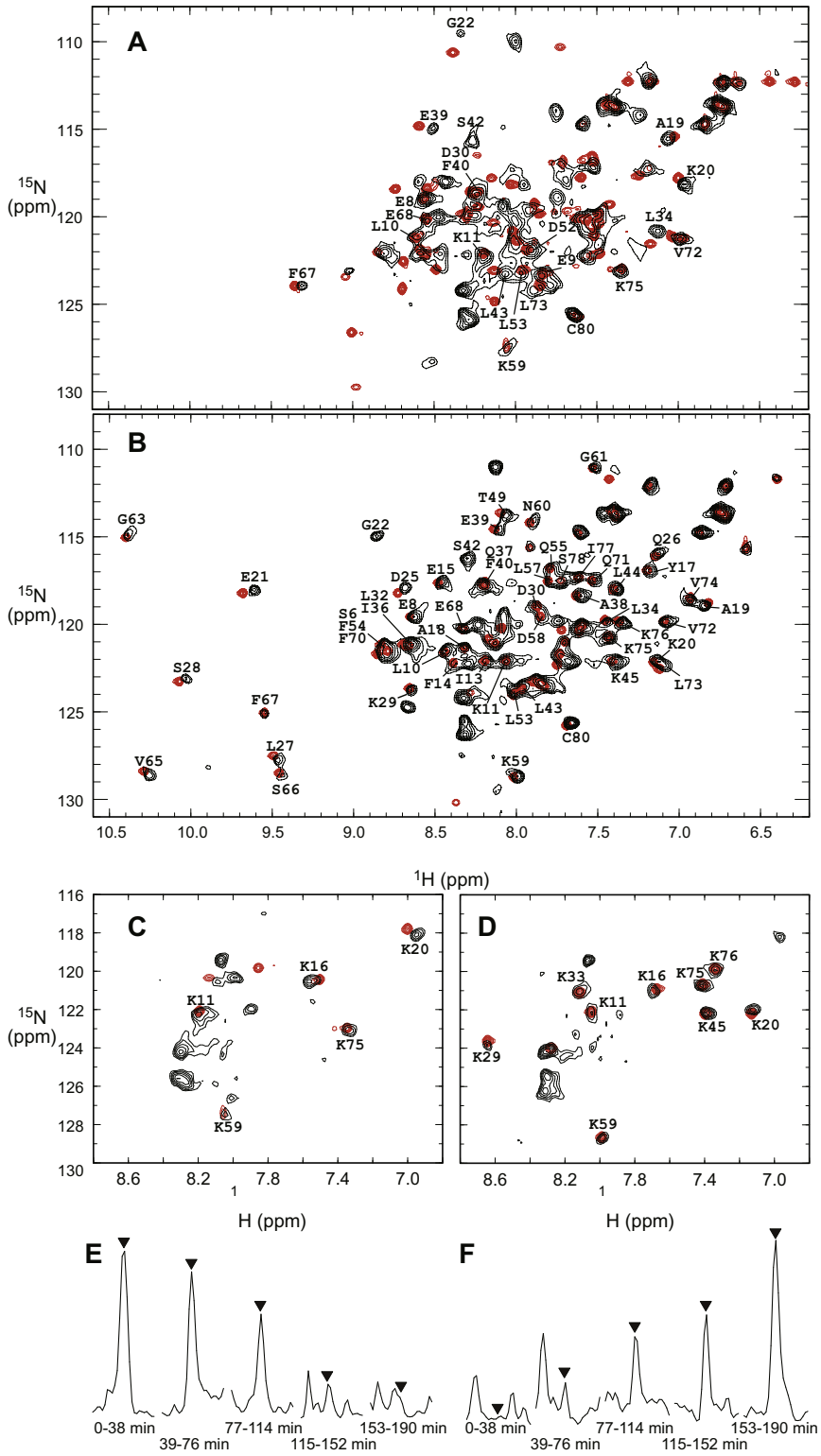

Fig. 2. Overlay of the 2D ^{1}H–^{15}N SOFAST–HMQC spectra of calbindin D_{9k} (P47M + C80) in HeLa cells (black) and the 2D ^{1}H–^{15}N HSQC spectra of calbindin D_{9k} (P47M + C80) *in vitro* (red). In the panels (A) and (B), the spectra of uniformly ^{15}N-labelled calbindin D_{9k} (P47M + C80) in HeLa cells which were obtained during the periods of 0–38 min (A) and 153 to 190 min (B) from the start of the in-cell NMR experiments were compared with uniformly ^{15}N-labelled calbindin D_{9k} (P47M + C80) in the Mg^{2+}- (A) and Ca^{2+}- (B) bound states *in vitro*. Likewise, in panels (C) and (D), the spectra of lysine-selectively ^{15}N-labelled calbindin D_{9k} (P47M + C80) in HeLa cells which were obtained during the periods of 0–38 min (C) and 153–190 min (D) from the start of the in-cell NMR experiments were compared with lysine-selectively ^{15}N-labelled calbindin D_{9k} (P47M + C80) in the Mg^{2+}- (C) and Ca^{2+}- (D) bound states *in vitro*. For each panel, cross-peaks in the in-cell NMR spectra are labelled with their corresponding backbone assignments. 1D cross sections of 2D ^{1}H–^{15}N SOFAST–HMQC spectra of lysine-selectively ^{15}N-labelled calbindin D_{9k} (P47M + C80) taken at the positions corresponding to the K75 residue in the Mg^{2+}- (E) and Ca^{2+}-bound state (F), indicating the time-dependent change in cross-peak intensity. Inverted triangles indicate the positions of the amide proton resonances due to the K75 residue.

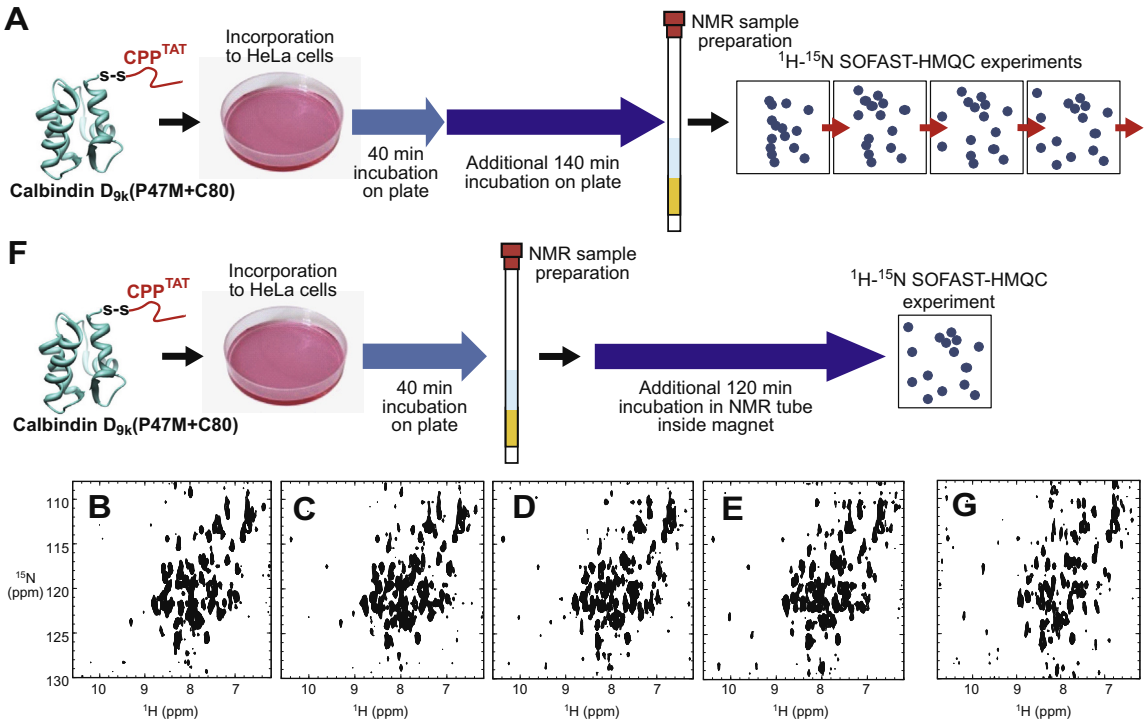

Fig. 3. (A) Schematic illustration of the in-cell NMR experiments of calbindin D_{9k} (P47M + C80) in HeLa cells with additional 140 min incubation on culture plates. (B–E) Time course of the 2D ^{1}H–^{15}N SOFAST–HMQC spectra of uniformly ^{15}N-labelled calbindin D_{9k} (P47M + C80) in HeLa cells obtained by employing the modified protocol shown in panel (A). The spectra were acquired during the period of 0–38 min (B), 39–76 min (C), 77–114 min (D), and 115–152 min (E) from the start of the in-cell NMR experiments. (F) Schematic illustration of the in-cell NMR experiments of calbindin D_{9k} (P47M + C80) in HeLa cells with additional 120 min incubation in NMR tube inside magnet. (G) The 2D ^{1}H–^{15}N SOFAST–HMQC spectrum of uniformly ^{15}N-labelled calbindin D_{9k} (P47M + C80) in HeLa cells obtained by employing the modified protocol shown in panel (F).

early stage (0–38 min from the start of the experiments) with the 2D ^{1}H–^{15}N HSQC spectra of the Mg^{2+}-bound calbindin D_{9k} (P47M + C80) *in vitro*. Although the number of observed ^{1}H–^{15}N correlation cross-peaks were less than expected, the cross-peak pattern has good agreement with that of the Mg^{2+}-bound state *in vitro*. In contrast, the cross-peaks observed on calbindin D_{9k} (P47M + C80) in HeLa cells in the later stages (114–152 min from the start of the experiments) (Fig. 2B and D) showed almost identical chemical shifts with the corresponding cross-peaks of Ca^{2+}-bound calbindin D_{9k} (P47M + C80) *in vitro*. First, these results demonstrated that the Ca^{2+} ions initially bound to the CPP^{TAT}-conjugated calbindin D_{9k} (P47M + C80) were released during the incorporation process into HeLa cells. This was confirmed by the similar in-cell NMR experiments employing the metal-free calbindin D_{9k} (P47M + C80) for the incorporation process, in which identical results were obtained (Supplementary Fig. S6).

Further our results showed that the calbindin D_{9k} (P47M + C80) just after the incorporation process binds Mg^{2+} ions. Time-dependence in signal intensity of representative cross-peaks suggested that the conversion from Mg^{2+}- to Ca^{2+}-bound states occurred continuously (Fig. 2E and F). To interpret this, we hypothesised that the Ca^{2+}-burst (presumably from the ER) happened continuously after the start of the in-cell NMR experiments, consequently the bound Mg^{2+} ions were replaced by Ca^{2+} ions, since the affinity of calbindin D_{9k} to Ca^{2+} is approximately 10^{3} times higher than Mg^{2+} [28]. In order to investigate when this Ca^{2+}-burst and the resulting time-dependent changes in calbindin D_{9k} (P47M + C80) start, we introduced an extra incubation time (120 min) in Dulbecco's Modified Eagle Medium, containing 10% fetal bovine serum and 1% antibiotics (penicillin/streptomycin) on the culture dish between the protein incorporation and the NMR sample preparation processes in the protocol (Fig. 3A). The additional incubation time caused no significant difference in in-cell NMR spectra (Fig. 3B–E), demonstrating that the time-dependent changes in the spectra do not start after the incorporation of calbindin D_{9k} (P47M + C80), but initiated after the NMR sample preparation process, in which HeLa cells were removed from the culture dish by trypsin/EDTA, washed and placed into an NMR tube.

Ca^{2+}-bursts occur in HeLa cells under various stresses [38–41]. It is known that NMR radio frequency (RF) pulses continuously move and reorient ions and polar molecules by an alternating electric field, and thereby increase the sample temperature. In order to verify the possibility that the RF pulses, and the resulting local temperature increase in HeLa cells, contribute to the increase of cytosolic Ca^{2+} concentration, we modified the protocol and left in-cell NMR samples inside the magnet for 120 min without applying any RF pulses before starting NMR measurements (Fig. 3F). The ^{1}H–^{15}N SOFAST–HMQC spectrum measured after this additional incubation time showed essentially an identical cross-peak pattern to that of the Ca^{2+}-bound state (Fig. 3G), suggesting that RF pulses are not the major cause for the increase in the cytosolic Ca^{2+} concentration.

4. Discussions

In this paper we established the method for and successfully monitored the increase in the concentration of cytosolic Ca^{2+} in HeLa cells by observing the time-dependent changes in the ^{1}H–^{15}N correlation cross-peaks of calbindin D_{9k} (P47M + C80). Our results demonstrated that metal ions bound to calbindin D_{9k} (P47M + C80) were released during the incorporation process, and that the this protein is initially in the Mg^{2+}-bound state. Then it was revealed that the continuous increase in the concentration of cytosolic Ca^{2+}, which is detected by the time-dependent change in the in-cell NMR spectra of calbindin D_{9k} (P47M + C80) from the Mg^{2+}- to Ca^{2+}-bound states, is autonomously induced as responses

to various stresses after NMR sample preparation. To the best of our knowledge, this is the first in-cell NMR report showing the stimulation-induced state-transition of proteins in living mammalian cells.

The existing protocols for eukaryotic in-cell NMR experiments are very effective for obtaining NMR spectra of proteins under specific/nonspecific intracellular interactions within a short time. However, as was demonstrated in this study, when investigating the behaviours of proteins involved in stress-induced responses or related to longer-term biological events, we have to examine carefully the stresses in the NMR tubes and resulting cell death. Improvements of NMR systems, aiming at keeping cells alive by e.g., recycling the media during NMR measurements, have been reported [42,43]. In the future, in-cell NMR studies in mammalian cells may head in the direction of achieving more "physiological" conditions during the experiments. In the method-development stage of mammalian in-cell NMR, the initial goal was to observe protein behaviours while cells are "alive" during the experiments. Once the approach matures, more detailed information on the conditions of host cells will become increasingly important for proper interpretation of observations by in-cell NMR. In this context, our method will provide a very useful tool for *in situ* monitoring of the "healthiness" of the cells in various in-cell NMR studies.

Acknowledgments

The authors thank Drs Markus Wälchli and Jonathan Heddle for the critical reading of the manuscript. This work was supported in part by the Funding Program for Next Generation World-Leading Researchers (NEXT Program) from Japan Society for the Promotion of Science (JSPS) and by the Asian Human Resources Fund of Tokyo Metropolitan Government (under Project Asian Net-work for Major Cities 21). DSSH thanks the scholarship from the Asian Human Resources Fund. JH thanks the Research Fellowship for Young Scientists (DC1) from JSPS.

Appendix A. Supplementary data

Supplementary data associated with this article can be found, in the online version, at http://dx.doi.org/10.1016/j.bbrc.2013.07.127.

References

[1] Z. Serber, A.T. Keatinge-Clay, R. Ledwidge, A.E. Kelly, S.M. Miller, V. Dötsch, High-resolution macromolecular NMR spectroscopy inside living cells, J. Am. Chem. Soc. 123 (2001) 2446–2447.
[2] R.J. Ellis, Macromolecular crowding: obvious but underappreciated, Trends Biochem. Sci. 26 (2001) 597–604.
[3] Z. Serber, L. Corsini, F. Durst, V. Dötsch, In-cell NMR spectroscopy, Methods Enzymol. 394 (2005) 17–41.
[4] S. Reckel, R. Hänsel, F. Löhr, V. Dötsch, In-cell NMR spectroscopy, Prog. Nucl. Magn. Reson. Spectrosc. 51 (2007) 91–101.
[5] D. Sakakibara, A. Sasaki, T. Ikeya, J. Hamatsu, T. Hanashima, M. Mishima, M. Yoshimasu, N. Hayashi, T. Mikawa, M. Walchli, B.O. Smith, M. Shirakawa, P. Güntert, Y. Ito, Protein structure determination in living cells by in-cell NMR spectroscopy, Nature 458 (2009) 102–105.
[6] Y. Ito, P. Selenko, Cellular structural biology, Curr. Opin. Struct. Biol. 20 (2010) 640–648.
[7] A.Y. Maldonado, D.S. Burz, A. Shekhtman, In-cell NMR spectroscopy, Prog. Nucl. Magn. Reson. Spectrosc. 59 (2011) 197–212.
[8] A.P. Schlesinger, Y. Wang, X. Tadeo, O. Millet, G.J. Pielak, Macromolecular crowding fails to fold a globular protein in cells, J. Am. Chem. Soc. 133 (2011) 8082–8085.
[9] C.A. Waudby, M.D. Mantle, L.D. Cabrita, L.F. Gladden, C.M. Dobson, J. Christodoulou, Rapid distinction of intracellular and extracellular proteins using NMR diffusion measurements, J. Am. Chem. Soc. 134 (2012) 11312–11315.
[10] P. Selenko, Z. Serber, B. Gade, J. Ruderman, G. Wagner, Quantitative NMR analysis of the protein G B1 domain in *Xenopus laevis* egg extracts and intact oocytes, Proc. Natl. Acad. Sci. USA 103 (2006) 11904–11909.
[11] T. Sakai, H. Tochio, T. Tenno, Y. Ito, T. Kokubo, H. Hiroaki, M. Shirakawa, In-cell NMR spectroscopy of proteins inside *Xenopus laevis* oocytes, J. Biomol. NMR 36 (2006) 179–188.
[12] K. Bertrand, S. Reverdatto, D.S. Burz, R. Zitomer, A. Shekhtman, Structure of proteins in eukaryotic compartments, J. Am. Chem. Soc. 134 (2012) 12798–12806.
[13] J. Hamatsu, D. O'Donovan, T. Tanaka, T. Shirai, Y. Hourai, T. Mikawa, T. Ikeya, M. Mishima, W. Boucher, B.O. Smith, E.D. Laue, M. Shirakawa, Y. Ito, High-resolution heteronuclear multidimensional NMR of proteins in living insect cells using a baculovirus protein expression system, J. Am. Chem. Soc. 135 (2013) 1688–1691.
[14] K. Inomata, A. Ohno, H. Tochio, S. Isogai, T. Tenno, I. Nakase, T. Takeuchi, S. Futaki, Y. Ito, H. Hiroaki, M. Shirakawa, High-resolution multi-dimensional NMR spectroscopy of proteins in human cells, Nature 458 (2009) 106–109.
[15] S. Ogino, S. Kubo, R. Umemoto, S. Huang, N. Nishida, I. Shimada, Observation of NMR signals from proteins introduced into living mammalian cells by reversible membrane permeabilization using a pore-forming toxin, streptolysin *o*, J. Am. Chem. Soc. 131 (2009) 10834–10835.
[16] L. Banci, L. Barbieri, I. Bertini, E. Luchinat, E. Secci, Y. Zhao, A.R. Aricescu, Atomic-resolution monitoring of protein maturation in live human cells by NMR, Nat. Chem. Biol. 9 (2013) 297–299.
[17] A.K. Campbell, Intracellular Calcium: Its Universal Role as Regulator, John Wiley & Sons Ltd, New York, 1983.
[18] M.J. Berridge, R.F. Irvine, Inositol trisphosphate, a novel second messenger in cellular signal transduction, Nature 312 (1984) 315–321.
[19] Y. Nishizuka, Studies and perspectives of protein kinase C, Science 233 (1986) 305–312.
[20] C. Cerella, M. Diederich, L. Ghibelli, The dual role of calcium as messenger and stressor in cell damage, death, and survival, Int. J. Cell. Biol. 2010 (2010) 546163.
[21] I. Kruman, Q. Guo, M.P. Mattson, Calcium and reactive oxygen species mediate staurosporine-induced mitochondrial dysfunction and apoptosis in PC12 cells, J. Neurosci. Res. 51 (1998) 293–308.
[22] B. Tombal, S.R. Denmeade, J.T. Isaacs, Assessment and validation of a microinjection method for kinetic analysis of $[Ca^{2+}]i$ in individual cells undergoing apoptosis, Cell Calcium 25 (1999) 19–28.
[23] G. Li, M. Mongillo, K.T. Chin, H. Harding, D. Ron, A.R. Marks, I. Tabas, Role of ERO1-alpha-mediated stimulation of inositol 1,4,5-triphosphate receptor activity in endoplasmic reticulum stress-induced apoptosis, J. Cell Biol. 186 (2009) 783–792.
[24] B.W. Schafer, C.W. Heizmann, The S100 family of EF-hand calcium-binding proteins: functions and pathology, Trends Biochem. Sci. 21 (1996) 134–140.
[25] P. Pinton, C. Giorgi, R. Siviero, E. Zecchini, R. Rizzuto, Calcium and apoptosis: ER-mitochondria Ca^{2+} transfer in the control of apoptosis, Oncogene 27 (2008) 6407–6418.
[26] D.E. Clapham, Calcium signaling, Cell 80 (1995) 259–268.
[27] L. Maler, J. Blankenship, M. Rance, W.J. Chazin, Site-site communication in the EF-hand Ca^{2+}-binding protein calbindin D_{9k}, Nat. Struct. Biol. 7 (2000) 245–250.
[28] B. Schwaller, Cytosolic Ca^{2+} buffers, Cold Spring Harb. Perspect. Biol. 2 (2010) a004051.
[29] W.J. Chazin, J. Kordel, T. Drakenberg, E. Thulin, P. Brodin, T. Grundstrom, S. Forsen, Proline isomerism leads to multiple folded conformations of calbindin D_{9k}: direct evidence from two-dimensional ^1H NMR spectroscopy, Proc. Natl. Acad. Sci. USA 86 (1989) 2195–2198.
[30] P. Schanda, E. Kupce, B. Brutscher, SOFAST–HMQC experiments for recording two-dimensional heteronuclear correlation spectra of proteins within a few seconds, J. Biomol. NMR 33 (2005) 199–211.
[31] J.C.J. Barna, E.D. Laue, M.R. Mayger, J. Skilling, S.J.P. Worrall, Exponential sampling, an alternative method for sampling in two-dimensional NMR experiments, J. Magn. Reson. 73 (1987) 69–77.
[32] P. Schmieder, A.S. Stern, G. Wagner, J.C. Hoch, Improved resolution in triple-resonance spectra by nonlinear sampling in the constant-time domain, J. Biomol. NMR 4 (1994) 483–490.
[33] T. Ikeya, A. Sasaki, D. Sakakibara, Y. Shigemitsu, J. Hamatsu, T. Hanashima, M. Mishima, M. Yoshimasu, N. Hayashi, T. Mikawa, D. Nietlispach, M. Walchli, B.O. Smith, M. Shirakawa, P. Güntert, Y. Ito, NMR protein structure determination in living *E. coli* cells using nonlinear sampling, Nat. Protoc. 5 (2010) 1051–1060.
[34] W.F. Vranken, W. Boucher, T.J. Stevens, R.H. Fogh, A. Pajon, M. Llinas, E.L. Ulrich, J.L. Markley, J. Ionides, E.D. Laue, The CCPN data model for NMR spectroscopy: development of a software pipeline, Proteins 59 (2005) 687–696.
[35] J. Kordel, N.J. Skelton, M. Akke, W.J. Chazin, High-resolution structure of calcium-loaded calbindin D_{9k}, J. Mol. Biol. 231 (1993) 711–734.
[36] N.J. Skelton, J. Kordel, W.J. Chazin, Determination of the solution structure of Apo calbindin D_{9k} by NMR spectroscopy, J. Mol. Biol. 249 (1995) 441–462.
[37] M. Akke, T. Drakenberg, W.J. Chazin, Three-dimensional solution structure of Ca^{2+}-loaded porcine calbindin D_{9k} determined by nuclear magnetic resonance spectroscopy, Biochemistry 31 (1992) 1011–1020.
[38] L.M. Pfeffer, I. Tamm, Interferon-beta inhibition of concanavalin A-stimulated calcium uptake and exchange in HeLa cells, J. Interferon Res. 6 (1986) 551–556.
[39] V.N. Bochkov, I.B. Cheglakov, D.E. Ligum, I. Gavrilov, P.V. Avdonin, Increase of calcium ion level in the cytoplasm of indo 1-loaded HeLa cells under the action of histamine, Biull. Eksp. Biol. Med. 109 (1990) 40–42.
[40] R.A. Riach, G. Duncan, M.R. Williams, S.F. Webb, Histamine and ATP mobilize calcium by activation of H1 and P2u receptors in human lens epithelial cells, J. Physiol. 486 (Pt 2) (1995) 273–282.
[41] T. Shinohara, T. Michikawa, M. Enomoto, J. Goto, M. Iwai, T. Matsu-ura, H. Yamazaki, A. Miyamoto, A. Suzuki, K. Mikoshiba, Mechanistic basis of

bell-shaped dependence of inositol 1,4,5-trisphosphate receptor gating on cytosolic calcium, Proc. Natl. Acad. Sci. USA 108 (2011) 15486–15491.
[42] N.G. Sharaf, C.O. Barnes, L.M. Charlton, G.B. Young, G.J. Pielak, A bioreactor for in-cell protein NMR, J. Magn. Reson. 202 (2010) 140–146.
[43] S. Kubo, N. Nishida, Y. Udagawa, O. Takarada, S. Ogino, I. Shimada, A gel-encapsulated bioreactor system for NMR studies of protein-protein interactions in living mammalian cells, Angew. Chem. Int. Ed. Engl. 52 (2013) 1208–1211.